Convergence Analysis of Code-Aided Channel Estimation by Means of Transfer Charts

Susanne Godtmann, Adrian Ispas, and Gerd Ascheid
Institute for Integrated Signal Processing Systems
RWTH Aachen University, Germany

***Abstract*— In this paper, we investigate the convergence behavior of code-aided channel estimation, also denoted as joint iterative channel estimation and decoding. A mutual information transfer chart is introduced in order to trace the information exchange between channel estimator and decoder throughout the iterative process.**

Furthermore, a heuristic concept to improve code-aided channel estimation is introduced that outperforms the classical concepts and has the major advantage that it allows for accurate convergence analysis.

I. Introduction

In order to cope with challenging synchronization issues in a low SNR environment, joint iterative synchronization and decoding is a promising approach to guarantee both, bandwidth efficiency and high synchronization accuracy [1]. Since the approach is based on feedback from the channel decoder, it is also referred to as code-aided synchronization.

Existing concepts for code-aided channel estimation typically rely on a posteriori information that is passed from the decoder output to the synchronization unit, e.g. [2], in order to improve the (channel) estimation and, subsequently, improve the decoding result. However, the question which type of decoder feedback yields the best results in terms of the coded BER, is not obvious. The classical approach based on the expectation maximization (EM) algorithm utilizes a posteriori decoder feedback [1] as also does the approach proposed in [3]. Algorithms that are based on factor graphs (FG) can use extrinsic decoder feedback. Another justification to use extrinsic feedback is to operate in accordance with the Turbo principle, since a Turbo decoder also makes use of extrinsic feedback. Examples for the utilization of a posteriori feedback and extrinsic feedback for code-aided channel estimation are [2],[3] and [4],[5], respectively.

In this paper, we introduce a heuristic type of decoder feedback which outperforms extrinsic and a posteriori decoder feedback in terms of the coded BER. It should be stressed that this is not in contradiction to the EM and the FG framework, since these frameworks have no claims on optimal convergence speed and, furthermore, rely on certain approximations.

The focus of this work is the study of convergence properties of code-aided channel estimation by means of mutual information transfer charts. Transfer charts are widely used in the context of the convergence analysis of concatenated codes [6]. Their applicability to code-aided channel estimation has already been investigated in e.g. [4] for extrinsic decoder feedback. For a posteriori feedback, transfer charts have been produced in [7]. However, there, the synchronizer transfer function can only be obtained by simulating the whole iterative system and tracing both its estimation accuracy (noted as ρ in [7]) and the mutual information (noted as I_{A_1} in [7]) throughout its iterations. Then, the transfer function can be generated based on this knowledge. However, it is desirable to obtain a prediction of the system behavior *without* the need to simulate the whole system.

In this paper, we investigate mutual information charts for extrinsic, a posteriori and the novel heuristic type of decoder feedback. We refrain from simulating the iterative system in order to obtain the transfer characteristics, but rely on a semi-analytical approach. Therefore, we derive the necessary probability density functions (pdf) of the log-likelihood ratios (LLR) at the output of the decoding and the synchronization unit for the case of imperfect channel state information (CSI). Furthermore, we show that the prediction of the mutual information at the synchronizer output for data-aided (initial) channel estimation, code-aided (iterative) channel estimation under the assumption of perfect feedback and perfect CSI can be calculated analytically. It is revealed that a precise prediction of the system behavior can be obtained when using the heuristic type of feedback, that was developed within this work. For the common case of a posteriori decoder feedback, accurate prediction can not be guaranteed for the general case, but only for the (important) second iteration.

II. Transmission System

The transmission model considered in this paper is depicted in Fig. 1. Information bits are grouped into packets of N bits, encoded with a convolutional code $\mathcal{C}$ of rate r_c, interleaved (Π) and mapped ($\mathcal{M}$) onto a BPSK modulation alphabet. Pilot symbols are then periodically inserted into the data symbol stream and transmitted over a flat Rayleigh fading channel that is also corrupted by additive white Gaussian noise (AWGN). A Jakes fading spectrum with normalized maximum Doppler frequency $F_d = f_d T$ is assumed, where T is the symbol duration.

Under the assumption of perfect symbol timing, the received baseband signal after matched filtering and sampling can be modeled as

$$y_k = h_k \cdot x_k + n_k, \tag{1}$$

where h_k is the complex fading coefficient at time instance k with $\mathrm{E}\left\{|h_k|^2\right\} = \sigma_h^2$, x_k is the transmitted symbol and n_k is a sample of complex-valued AWGN with independent real and imaginary part, each having zero-mean and variance $N_0/(2E_s)$.

A. Ispas is now with the Commun. Technology Laboratory, ETH Zürich.
S. Godtmann thanks the Deutsche Telekom Stiftung for its financial support.

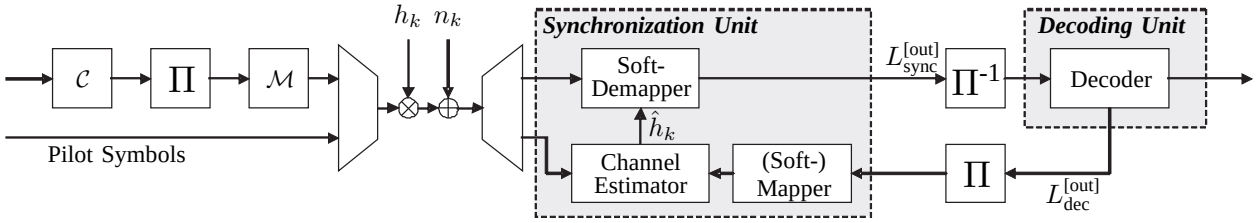

Figure 1. Transmission System

At receiver side, the received data sample are corrected with channel estimates that are obtained via a Wiener filter process [8] and the subsequently demapped coded bits are deinterleaved and then decoded. As opposed to a classical pilot symbol assisted system (PSAM) [9], [10], where only pilot symbols contribute to the channel estimate, data symbols are fed back from the decoding unit and used to obtain unmodulated received samples - also called channel observations. The number of channel observations, therefore, increases as compared to the classical PSAM system and can contribute to an improved channel estimate that is then used in the next iteration for correction.

III. Code-Aided Channel Estimation

For code-aided channel estimation, information feedback of the channel decoder is used in order to estimate the transmitted symbols and, with the help of these, the channel. However, it is not straightforward to obtain a (feasible) optimum code-aided channel estimator. However, for the case of no feedback from the decoder (initial channel estimation) and the case of perfect feedback from the decoder, the noise on the channel observations is Gaussian. Hence, the LMMSE channel estimator is optimum [8]. Therefore, in accordance with e.g. [2], we here consider LMMSE channel estimation also for the case of imperfect feedback from the decoder and calculate the filter coefficients as if the feedback were perfect.

For the observation of the channel $\tilde{h}_k$ at the data symbol positions, we then get

$$\tilde{h}_k = y_k \cdot \hat{\alpha}_k^* = h_k \cdot x_k \cdot \hat{\alpha}_k^* + n_k \cdot \hat{\alpha}_k^*, \tag{2}$$

where α_k denotes the (soft) estimate of the transmitted symbol at time instant k, which can be calculated as [1]

$$\alpha_k = \sum_{x \in \mathcal{X}} x \ \Pr\left(x_k = x | \boldsymbol{y}, \hat{h}_k^{[n-1]}\right), \tag{3}$$

where $\hat{h}_k^{[n-1]}$ denotes the channel estimate at time instance k from the previous iteration. The soft-symbols α_k depend on the a posteriori probabilities $\Pr\left(x_k = x | \boldsymbol{y}, \hat{h}_k^{[n-1]}\right)$. The soft information provided by the MAP decoder can be used here. Instead of choosing the a posteriori output of the MAP decoder as input for the soft-symbol calculation, it is also possible to use the extrinsic decoder output, as e.g. pursued in [4]. The extrinsic decoder output LLRs are denoted as $L_{\text{dec}}^{[\text{out,ex}]}$, whereas the a posteriori decoder output LLRs are denoted as $L_{\text{dec}}^{[\text{out,ap}]}$ in the sequel.

For the (offline) calculation of the Wiener filter coefficients, in accordance with other published work, we assume perfect feedback from the decoder. Therefore, the calculation is similar as in [9], except that all data symbols are treated like pilot symbols. The filter length for the iterative estimation is denoted as f_l^{itr}. Furthermore, it should be mentioned that - in accordance with [4] - the channel observation $\tilde{h}_k$ at time instant k does not contribute to the estimate $\hat{h}_k$.

A. EXTpINIT Feedback

We have seen that mainly two options of decoder feedback exist in the literature: extrinsic feedback and a posteriori feedback. In this subsection, we introduce a new (heuristic) type of feedback which outperforms the two other feedback types in terms of the coded bit error rate.

We propose the following modification: Instead of using only the extrinsic LLRs, that are present at the output of the decoder, the LLRs that are present at the output of the soft-demapper after the very first iteration are added to the extrinsic values. The composed LLRs are denoted as $L_{\text{dec}}^{[\text{out,EpI}]}$ in the following and we label this feedback type EXTpINIT feedback. An intuitive motivation for this approach is that only new ,i.e. extrinsic, information and valuable non-distorted information form the initial (data-aided) channel estimation is passed on. Therefore, the iterative receiver can forget previous erroneous decoder feedback, which is surely an advantage.

Fig. 2 depicts the coded BER versus the pilot spacing for the three described types of decoder feedback: extrinsic feedback (circular markers), a posteriori feedback (hexagram markers) and EXTpINIT feedback (square markers). The results are depicted after the first, fifth and tenth iteration. The BER for perfect feedback, which corresponds to the knowledge of all transmitted symbols and for perfect CSI are represented by the dashed line and the dashed-dotted line, respectively. The results reveal that code-aided channel estimation also allows for accurate results, if the pilot spacing does not obey the Nyquist rate of the time-variant channel fading process. For the case of large pilot spacings, we can see that the heuristical EXTpINIT concept performs best. A posteriori feedback also works well, but extrinsic feedback is significantly outperformed by the two other feedback types. As already stated in the introduction, the fact that EXTpINIT feedback performs best is not in contradiction to the theoretical frameworks that justify extrinsic and a posteriori feedback, respectively, since these frameworks do not claim optimum convergence speed.

IV. Convergence Analysis

In this section, we present a mutual information transfer chart that is able to track the convergence of (iterative) code-aided synchronization.

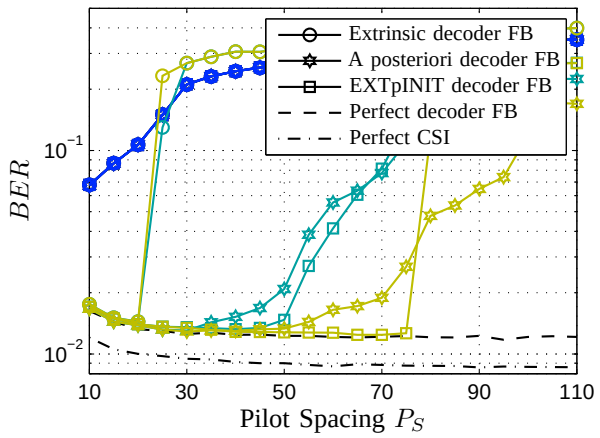

Figure 2. BER vs. P_S for diff. types of decoder feedback, $N = 250002$, $F_d = 0.02$, {1,5,10} Iterations, $E_b/N_0 = 5$ dB, BPSK, $(5,7)_8$ systematic code, $r_c = 1/2$, $f_l^{\text{ini}} = 10$, $f_l^{\text{itr}} = 100$

We are interested in tracking the mutual information between the encoded BPSK symbol X and its corresponding LLR value L, that evolves during the iterative process. Under the assumption that $X=-1$ and $X=+1$ are equally likely and that $p(\xi|X) = p(-\xi|-X)$ holds, the corresponding mutual information is given as [6]:

$$I(X;L) = 1 - \int_{-\infty}^{\infty} p(\xi|X=+1)\, \log_2\left[1+\exp\left(-\xi\right)\right] d\xi, \quad (4)$$

where ξ is the realization of the LLR.

In order to evaluate (4) analytically, it is necessary to know the pdf of the LLRs. Therefore, we are interested in calculating $p(\xi|x)$, where x is the BPSK symbol. Note that the results are straightforward to extend to other modulation schemes.

A. Pdf of LLRs at Synchronizer Output

For a flat Rayleigh fading channel and imperfect CSI, $p(\xi|x)$ can be obtained as

$$p_{L_{\text{sync}}^{[\text{out}]}}(\xi|x) = \int_0^{\infty} p(\hat{a})\; p_{L_{\text{sync}}^{[\text{out}]}}(\xi|x,\hat{a})\; d\hat{a}, \quad (5)$$

where $\hat{a}$ is defined as $|\hat{h}|$. In order to obtain $p_{L_{\text{sync}}^{[\text{out}]}}(\xi|x,\hat{a})$, we make use of the pdf of the received data sample y given the LMMSE fading estimate $\hat{h}$

$$p(y|x,\hat{h}) = \frac{1}{\pi(\sigma_n^2+\sigma_{c,p}^2)} \cdot \exp\left(-\frac{|y-\hat{h}\cdot x|^2}{\sigma_n^2+\sigma_{c,p}^2}\right), \quad (6)$$

where $\sigma_{c,p}^2$ is the variance of the estimation error at position p between two adjacent pilot symbols, $p \in \{1,\ldots,P_S-1\}$. It is shown in the first appendix that $p_{L_{\text{sync}}^{[\text{out}]}}(\xi|x,\hat{a}) = p_{L_{\text{sync}}^{[\text{out}]}}(\xi|x,\hat{h})$ and that it is Gaussian with

$$p_{L_{\text{sync}}^{[\text{out}]}}(\xi|x,\hat{a}) = \mathcal{N}\left(\frac{4\cdot\hat{a}^2}{\sigma_n^2+\sigma_{c,p}^2}\cdot x, \frac{8\cdot\hat{a}^2}{\sigma_n^2+\sigma_{c,p}^2}\right). \quad (7)$$

In case the inverse of the pilot spacing satisfies the Nyquist rate of the channel process, i.e. $P_S < 1/(2\cdot F_d)$, $\sigma_{c,p}^2$ does no longer depend on p, cf. [11], i.e. $\sigma_{c,p}^2 = \sigma_c^2$ for all p. (This only holds formally for an infinite observation interval, but is also a valid approximation for finite observation intervals.) It should be stressed that for the case of initial LMMSE channel estimation and LMMSE channel estimation with perfect feedback, $\sigma_{c,p}^2$ can be calculated analytically. In case of imperfect feedback, it needs to be approximated. A suitable approximation is discussed in Section IV-D.2.

Solving (5) with the help of [12] (3.325) yields:

$$p_{L_{\text{sync}}^{[\text{out}]}}(\xi|x) = \frac{\sigma_n^2+\sigma_{c,p}^2}{4\sqrt{\left(\sigma_h^2-\sigma_{c,p}^2\right)\left(\sigma_h^2+\sigma_n^2\right)}} \cdot \exp\left(\frac{x\cdot\xi}{2} - \frac{|\xi|}{2}\sqrt{\frac{\sigma_h^2+\sigma_n^2}{\sigma_h^2-\sigma_{c,p}^2}}\right). \quad (8)$$

B. Pdf of LLRs at Decoder Output

In [6], the extrinsic decoder LLRs of a BCJR decoder, e.g. a log-MAP decoder, are modeled with a Gaussian pdf according to

$$p_{L_{\text{dec}}^{[\text{out,ex}]}}(\xi|x) = \mathcal{N}\left(\frac{(\sigma_{\text{dec}}^{\text{ext}})^2}{2}\cdot x, (\sigma_{\text{dec}}^{\text{ext}})^2\right). \quad (9)$$

Even though this is a very commonly made assumption - almost all literature on EXIT charts relies on this - it is not necessarily true, especially not if the decoder input results from a fading channel.

However, to the best of our knowledge, this is the best available model in the literature. Therefore, we also choose to approximate the pdf for the extrinsic decoder feedback by (9). For the case of EXTpINIT decoder feedback, the addition of the LLRs after the very first iteration, can be considered a static input into the synchronizer unit. It is, therefore, not necessary to consider it during the tracking of the mutual information, since it is constant throughout the iterations. Therefore, we can make use of (9) for convergence analysis.

The interesting question is now regarding the pdf of $L_{\text{dec}}^{[\text{out,ap}]}$. Due to the characteristic of extrinsic information, in accordance with e.g. [13], the extrinsic decoder LLRs $L_{\text{dec}}^{[\text{out,ex}]}$ can be assumed to be independent of the interleaved synchronizer output LLRs $L_{\text{sync}}^{[\text{out}]}$. Therefore, we can compute the pdf $p_{L_{\text{dec}}^{[\text{out,ap}]}}(\xi|x)$ from (8) and (9) as

$$p_{L_{\text{dec}}^{[\text{out,ap}]}}(\xi|x) = p_{L_{\text{sync}}^{[\text{out}]}}(\xi|x) \;*\; p_{L_{\text{dec}}^{[\text{out,ex}]}}(\xi|x), \quad (10)$$

where $*$ denotes the convolution. The evaluation of (10) requires a lot of algebra. Due to space constraints, we just give the result:

$$p_{L_{\text{dec}}^{[\text{out,ap}]}}(\xi|x) = \frac{f}{2}\exp\left(\frac{(\sigma_{\text{dec}}^{\text{ext}})^2}{2}\left(g^2-\frac{1}{4}\right)+\frac{x\cdot\xi}{2}\right) \cdot\left[\exp\left(g\xi\right)\;\text{erfc}\left(\frac{\sigma_{\text{dec}}^{\text{ext}}}{\sqrt{2}}g+\frac{\xi}{\sqrt{2}\sigma_{\text{dec}}^{\text{ext}}}\right) + \exp\left(-g\xi\right)\;\text{erfc}\left(\frac{\sigma_{\text{dec}}^{\text{ext}}}{\sqrt{2}}g-\frac{\xi}{\sqrt{2}\sigma_{\text{dec}}^{\text{ext}}}\right)\right], \quad (11)$$

with

$$f = \frac{\sigma_n^2+\sigma_{c,p}^2}{4\sqrt{(\sigma_h^2+\sigma_n^2)(\sigma_h^2-\sigma_{c,p}^2)}} \quad \text{and} \quad g = \frac{1}{2}\sqrt{\frac{\sigma_h^2+\sigma_n^2}{\sigma_h^2-\sigma_{c,p}^2}}.$$

The structure of (11) is similar to the result given in [6], Eq. (45) for perfect CSI. In order to further demonstrate the correctness of (11) and the validity of the assumption made in (9) and (10), please refer to Fig. 3.

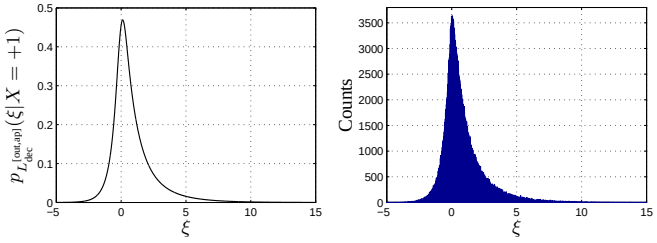

(a) Plot of Equation (11) (b) Histogram (from simulation)

Figure 3. Pdf of $L_{\text{dec}}^{[\text{out,ap}]}$; $N = 2.5 \cdot 10^5$, $F_d = 0.02$, $P_S = 50$, $E_b/N_0 = 4\,\text{dB}$, $(5,7)_8$ systematic code, $r_c = 1/2$, $f_l^{\text{ini}} = 10$

C. Obtaining the Decoder Transfer

We obtain the decoder transfer the same way as in, e.g. [13], i.e. assuming the LLRs at the decoder input to be Gaussian distributed. Even though this is not true, cf. (8), this simplification has been widely used in the literature. Results not depicted here reveal that the decoder transfers for both cases almost coincide. The Gaussian assumption has the advantage that the decoder transfer is independent of the channel.

D. Obtaining the Synchronizer Transfer

1) Extrinsic and EXTpINIT Decoder Feedback: In case we use extrinsic decoder feedback or EXTpINIT decoder feedback as input to the synchronizer, i.e. $L_{\text{sync}}^{[\text{in}]} = L_{\text{dec}}^{[\text{out,ex}]}$ or $L_{\text{sync}}^{[\text{in}]} = L_{\text{dec}}^{[\text{out,EpI}]}$, the generation of the input LLRs in order to evaluate the behavior of the synchronizer transfer is straightforward. The extrinsic decoder LLRs are generated as random variable according to (9). The parameter that determines the input mutual information $\mathcal{I}(X; L_{\text{sync}}^{[\text{in}]}) = \mathcal{I}(X; L_{\text{dec}}^{[\text{out,ex}]})$ is the variance of the extrinsic decoder LLRs $(\sigma_{\text{dec}}^{\text{ext}})^2$. Thus, one obtains $\mathcal{I}(X; L_{\text{dec}}^{[\text{out,ex}]}) = J((\sigma_{\text{dec}}^{\text{ext}})^2)$ and it follows

$$(\sigma_{\text{dec}}^{\text{ext}})^2 = J^{-1}(\mathcal{I}(X; L_{\text{dec}}^{[\text{out,ex}]})), \tag{12}$$

where $J(\cdot)$ is defined as in [6]. With this result the extrinsic decoder LLRs can be generated as a function of the input mutual information $\mathcal{I}(X; L_{\text{sync}}^{[\text{in}]})$.

2) A posteriori Decoder Feedback: Things get fairly more complicated for a posteriori decoder feedback. As the synchronizer input is determined by (11), which depends on $(\sigma_{\text{dec}}^{\text{ext}})^2$ and $\sigma_{c,p}^2$, the relation between $(\sigma_{\text{dec}}^{\text{ext}})^2$ and $\sigma_{c,p}^2$ needs to be known. Since $\sigma_{c,p}^2$ depends on the synchronizer output of the previous iteration, the knowledge of the decoder transfer is indispensable (cf. Section IV-C) to find the relation between $(\sigma_{\text{dec}}^{\text{ext}})^2$ and $\sigma_{c,p}^2$. Hence, for a posteriori feedback it is impossible to analyze the performance of the synchronization and decoding unit separately with a two-dimensional transfer chart.

Nevertheless, with the help of the decoder transfer, the decoder input mutual information $\mathcal{I}(X; L_{\text{dec}}^{[\text{in}]})$ is obtained from the synchronizer input mutual information $\mathcal{I}(X; L_{\text{sync}}^{[\text{in}]})$. For a given AWGN σ_n^2, the synchronizer output of the previous iteration $\mathcal{I}(X; L_{\text{dec}}^{[\text{in}]}) = \mathcal{I}(X; L_{\text{sync}}^{[\text{out}]})$ is a function of $\sigma_{c,p}^2$, i.e. $\mathcal{I}(X; L_{\text{dec}}^{[\text{in}]}) = J(\sigma_{c,p}^2)$.

Instead of calculating $\sigma_{c,p}^2$ by inversion, a heuristic model is used. The major advantage of such a heuristic model is the possibility to model the MSE as dependent on the position p of a data symbol between the two adjacent pilot symbols. If we had chosen to calculate the inversion, a constant $\sigma_{c,p}^2 = \sigma_c^2$ would have had to be assumed. The heuristic MSE is modeled according to

$$MSE = MSE_{\text{ana}}^{\text{ini}}(p) \cdot \left(\frac{MSE_{\text{ana}}^{\text{itr}}}{MSE_{\text{ana}}^{\text{ini}}(p)} \right)^{\eta}, \tag{13}$$

where $MSE_{\text{ana}}^{\text{ini}}(p)$ and $MSE_{\text{ana}}^{\text{itr}}$ denote the analytical MSE for initial estimation (PSAM) at position p and the analytical MSE for the case of perfect feedback. The exponent η is defined as

$$\eta = \frac{\mathcal{I}(X; L_{\text{dec}}^{[\text{in}]}) - \mathcal{I}(X; L_{\text{sync}}^{[\text{out,ini}]})}{\mathcal{I}(X; L_{\text{sync}}^{[\text{out,pf}]}) - \mathcal{I}(X; L_{\text{sync}}^{[\text{out,ini}]})}, \tag{14}$$

where $L_{\text{sync}}^{[\text{out,pf}]}$ denotes the synchronizer output LLRs for the case of perfect decoder feedback and $L_{\text{sync}}^{[\text{out,ini}]}$ for the case of no decoder feedback, respectively. The model is chosen such that it is exact for the case of no feedback and for the case of perfect feedback.

The mutual information at the synchronizer input can then be calculated as

$$\mathcal{I}(X; L_{\text{sync}}^{[\text{in}]}) = \mathcal{I}(X; L_{\text{dec}}^{[\text{out,ap}]}) = \frac{1}{P_S - 1} \sum_p J_p\left(\sigma_{c,p}^2, (\sigma_{\text{dec}}^{\text{ext}})^2\right),$$

where

$$J_p\left(\sigma_{c,p}^2, (\sigma_{\text{dec}}^{\text{ext}})^2\right) = 1 - \int_{-\infty}^{\infty} p_{L_{\text{dec}}^{[\text{out,ap}]}}(\xi|X=+1)\, \log_2\left[1+\exp(-\xi)\right] d\xi$$

and $p_{L_{\text{dec}}^{[\text{out,ap}]}}(\xi|X=+1)$ is defined according to (11). Hence, the mutual information is calculated for every position p and then averaged over all positions.

In order to evaluate the synchronizer transfer, we generate the random variables that represent input LLRs as follows:

$$L_{\text{sync}}^{[\text{in}]} = L_{\text{dec}}^{[\text{out,ap}]} = L_{\text{sync}}^{[\text{out}]} + L_{\text{dec}}^{[\text{out,ex}]}, \tag{15}$$

where $L_{\text{sync}}^{[\text{out}]}$ can be modeled according to (17).

The fading estimate $\hat{h}_\upsilon$ in (17) can be written as $\hat{h}_\upsilon = h_\upsilon + c_\upsilon$, where $(\cdot)_\upsilon$ denotes the real or imaginary part. It is shown in the second appendix, that c_υ can be modeled as a Gaussian random variable according to (21).

To sum up this subsection: It is feasible to approximate the synchronizer transfer for a posteriori decoder feedback, but there are a lot of possibly erroneous assumptions, i.e. correlations between synchronizer and decoder can exist but are not considered, the channel estimation error is not Gaussian distributed for imperfect decoder feedback, the channel estimation error is modeled artificially (cf. (13)). Furthermore, the synchronizer transfer indispensably depends on the decoder transfer, which makes its generation complicated and computationally complex.

V. Simulation Results

In this section, we investigate the accuracy of the mutual information transfer chart developed in Section IV for three types of decoder feedback.

We investigate the scenario of a flat Rayleigh fading channel with maximum normalized Doppler spread $F_d = 0.02$. The spectrum of the channel fading process is determined by the Jakes Model. The pilot spacing is chosen to $P_S = 20$ for extrinsic decoder feedback (obeys Nyquist rate) and $P_S = 50$ for a posteriori decoder feedback and EXTpINIT feedback (below Nyquist rate). The reason why a less hostile environment is chosen for extrinsic feedback is that otherwise convergence could not be observed. The block length is $N = 2.5 \cdot 10^5$ and $E_b/N_0 = 5\,\text{dB}$. As initial filter length we choose $f_l^{\text{ini}} = 10$ and for the filter length of the iterative LMMSE filter $f_l^{\text{itr}} = 100$. As decoder, we use the typical maximum-a-posteriori (MAP) decoder. Note that the parameters are chosen as for the results depicted in Fig. 2 and that the qualitative behavior of the transfer charts does not change if other scenarios, e.g. higher SNR, are considered.

The results for the convergence analysis are depicted in Fig. 4. The dashed lines correspond to the semi-analytical results for $\mathcal{I}_{\text{dec}}^{[\text{out}]} = 0$ and $\mathcal{I}_{\text{dec}}^{[\text{out}]} = 1$, the dashed dotted line represents the case of perfect CSI. It should be stressed that these values can also be obtained analytically by making use of (8) and evaluating (4) ('*' and 'o' markers). Note that the markers perfectly coincide with the dashed and dashed dotted lines. Let us now first examine the case of extrinsic decoder feedback (cf. Fig. 4 (a)). The prediction of the system behavior (transfer functions) matches well the real system behavior (10 trajectories are plotted). However, a closer look reveals small inaccuracies, where the inaccuracy in the prediction of the decoder output is due to the reasons given in Section IV-C. The inaccuracy in the prediction of the synchronizer transfer is mostly connected to the erroneous assumption of a Gaussian distributed decoder output. Regarding the case of EXTpINIT feedback, one can say that despite the small inaccuracy in the prediction of the decoder output (due to Section IV-C), the prediction is fairly accurate. Referring to a posteriori decoder feedback, cf. Fig. 4 (c), the prediction of the synchronizer output does not work at all, except for the second iteration. This is due to the erroneous assumptions that needed to be made in Section IV-D.2. Note that the decoder transfer in Fig. 4 (c) is different to the two other decoder transfers. This is due to the fact that in Fig. 4 (c) a-posteriori information and not extrinsic information is traced.

The results up to now reveal that the prediction of the system behavior by means of transfer charts works well for extrinsic decoder feedback and EXTpINIT decoder feedback. Even though it fails for a posteriori feedback, the method still allows an accurate prediction for the very important second iteration. It is the difference between the mutual information after the first iteration and after the second iterations that triggers the convergence of code-aided channel estimation. It might not be possible to predict the number of necessary iterations for a posteriori feedback accurately, but it is possible to obtain an indication whether the system converges or not. The results are depicted in Fig. 5. The predicted gain is normalized to the maximum achievable gain:

$$\Delta\mathcal{I}_{\text{sync}}^{\text{gain,2nd}} = \frac{\mathcal{I}(X; L_{\text{sync}}^{[\text{out,2nd}]}) - \mathcal{I}(X; L_{\text{sync}}^{[\text{out,ini}]})}{\mathcal{I}(X; L_{\text{sync}}^{[\text{out,pf}]}) - \mathcal{I}(X; L_{\text{sync}}^{[\text{out,ini}]})}, \tag{16}$$

As already mentioned, $\mathcal{I}(X; L_{\text{sync}}^{[\text{out,ini}]})$ and $\mathcal{I}(X; L_{\text{sync}}^{[\text{out,pf}]})$ can be calculated analytically. In Fig. 5 (a) it becomes obvious, why extrinsic feedback performs so poorly (cf. Fig. 2). The gain even becomes negative for pilot spacings larger than 25. Comparing Fig. 5 (b) with Fig. 5 (c) and keeping in mind the two similar concepts, reveals that the actual system behavior till the second iteration is the same for EXTpINIT feedback and a posteriori decoder feedback. However, evidently, prediction works more accurately with the concept introduced in Section IV-D.1.

VI. Conclusion

In this paper, we have investigated code-aided channel estimation for a flat Rayleigh fading channel. In this context, we considered two typical types of decoder feedback: extrinsic and a posteriori. It is shown that a posteriori feedback outperforms extrinsic feedback. Additionally, we introduce a third type of decoder feedback, called EXTpINIT feedback. This feedback type is heuristical, but outperforms extrinsic and a posteriori feedback in some scenarios.

In order to trace the convergence of code-aided channel estimation, we derive the pdf of the synchronizer output and the decoder output for the case of imperfect CSI. With the help of these pdfs, it is possible to trace the convergence behavior for extrinsic and EXTpINIT decoder feedback using a mutual information transfer chart. It has furthermore been demonstrated that predicting the convergence behavior for a posteriori decoder feedback is fairly complicated and, additionally, fairly inaccurate. It is solely precise for the second iteration.

Independent of the decoder feedback type, we show that the mutual information at the synchronizer output for initial channel estimation, code-aided channel estimation under the assumption of perfect feedback and perfect CSI can be calculated analytically.

Appendix I

Here, it is shown that $p_{L_{\text{sync}}^{[\text{out}]}}(\xi|x,\hat{h}) = p_{L_{\text{sync}}^{[\text{out}]}}(\xi|x,\hat{a})$ and that it is Gaussian. From (6), we get

$$\begin{aligned} L_{\text{sync}}^{[\text{out}]} &= \log\frac{p(y|x=+1,\hat{h})}{p(y|x=-1,\hat{h})} \\ &= \frac{1}{\sigma_n^2+\sigma_{c,p}^2}\left(|y-\hat{h}|^2 - |y+\hat{h}|^2\right) = \frac{4}{\sigma_n^2+\sigma_{c,p}^2}\Re\{\hat{h}^* y\} \\ &= \frac{4}{\sigma_n^2+\sigma_{c,p}^2}\left[|\hat{h}|^2 x + \hat{h}_I\left(-c_I x + n_I\right) + \hat{h}_Q\left(-c_Q x + n_Q\right)\right] \end{aligned} \tag{17}$$

$$= \frac{4}{\sigma_n^2+\sigma_{c,p}^2}\left(|\hat{h}|^2 \cdot x + |\hat{h}| \cdot n_t\right), \tag{18}$$

with $n_t \sim \mathcal{N}\left(0, (\sigma_n^2+\sigma_{c,p}^2)/2\right)$ and c denoting the estimation error. $(\cdot)_I$ and $(\cdot)_Q$ denote the real and imaginary part of $(\cdot)$.

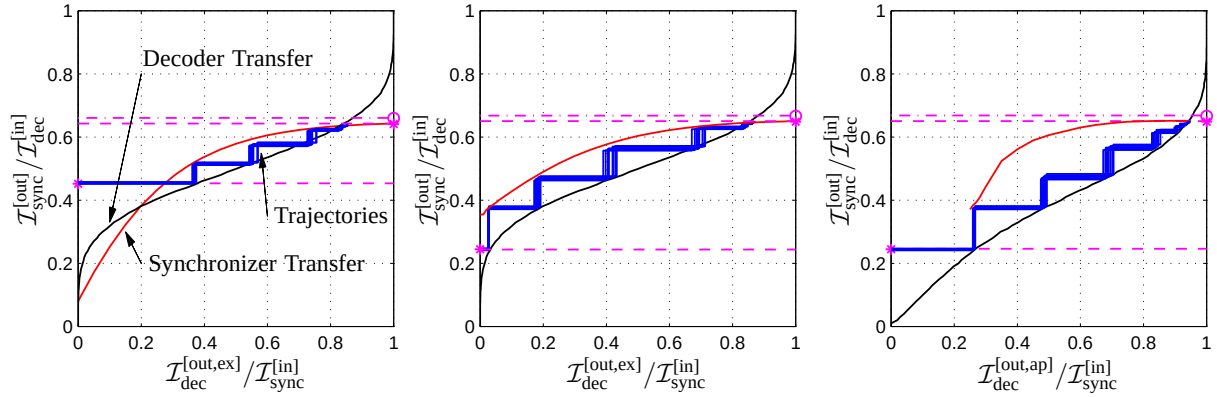

(a) Extrinsic decoder feedback, $P_S = 20$ (b) EXTpINIT decoder feedback, $P_S = 50$ (c) A posteriori decoder feedback, $P_S = 50$

Figure 4. Transfer charts; $N = 2.5 \cdot 10^5$, $F_d = 0.02$, $E_b/N_0 = 5\,\text{dB}$, $(5,7)_8$ systematic code, $r_c = 1/2$, $f_l^{\text{ini}} = 10$, $f_l^{\text{itr}} = 100$, 10 frames

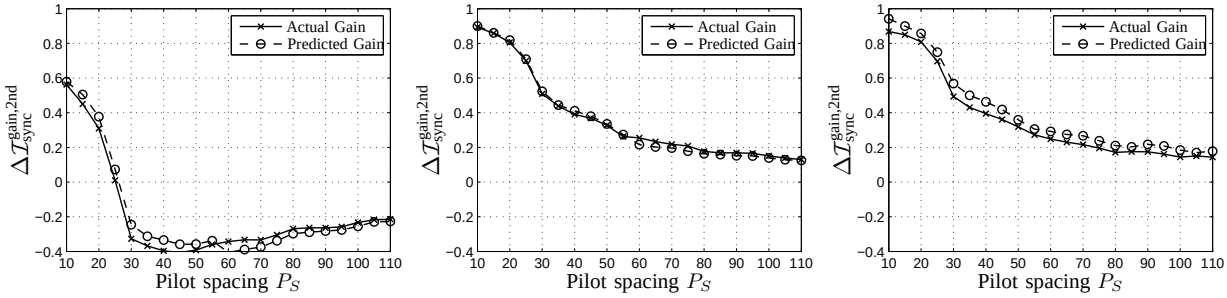

(a) Extrinsic decoder feedback (b) EXTpINIT decoder feedback (c) A posteriori decoder feedback

Figure 5. Gain of $\mathcal{I}(X; L_{\text{sync}}^{[\text{out}]})$ at the 2nd iteration ($\Delta\mathcal{I}_{\text{sync}}^{\text{gain,2nd}}$) vs. pilot spacing;
$N = 2.5 \cdot 10^5$, $F_d = 0.02$, $E_b/N_0 = 5\,\text{dB}$, $(5,7)_8$ systematic code, $r_c = 1/2$, $f_l^{\text{ini}} = 10$, $f_l^{\text{itr}} = 100$

APPENDIX II

The real or imaginary component of the fading estimate can be written as $\hat{h}_\upsilon = h_\upsilon + c_\upsilon$. In this appendix, we calculate the pdf $p_\upsilon(c_\upsilon|h_\upsilon)$. According to Bayes' rule, we write:

$$p(c_\upsilon|h_\upsilon) = p(c_\upsilon, h_\upsilon)/p(h_\upsilon). \tag{19}$$

$p(h_\upsilon)$ is Gaussian distributed with variance $\sigma_h^2/2$ and $p(c_\upsilon, h_\upsilon)$ is determined by a bivariate Gaussian distribution with the correlation coefficient:

$$\rho_p = \frac{\mathrm{E}\{c_\upsilon \cdot h_\upsilon\}}{\sqrt{\mathrm{E}\{c_\upsilon^2\} \cdot \mathrm{E}\{h_\upsilon^2\}}} = 2 \cdot \frac{\mathrm{E}\{c_\upsilon \cdot (\hat{h}_\upsilon - c_\upsilon)\}}{\sigma_{c,p} \cdot \sigma_h}. \tag{20}$$

Due to the concept of LMMSE channel estimation, (20) simplifies to $\rho_p = -\sigma_{c,p}/\sigma_h$. Evaluating (19) then yields:

$$p(c_\upsilon|h_\upsilon) = \mathcal{N}\left(\frac{\rho_p h_\upsilon \sigma_{c,p}}{\sigma_h}, (1-\rho_p^2)\frac{\sigma_{c,p}^2}{2}\right). \tag{21}$$

c_υ can, therefore, be written as

$$c_\upsilon = -h_\upsilon \cdot \sigma_{c,p}^2/\sigma_h^2 + e_\upsilon. \tag{22}$$

In order to make sure that c_υ is appropriately correlated with its previous/future values, the temporal correlation of the zero-mean Gaussian random variable e_υ is modeled similarly to h_υ.

REFERENCES

[1] N. Noels, H. Steendam, and M. Moeneclaey, "Carrier and clock recovery in (turbo) coded systems: Cramér-rao bound and synchronizer performance," *EURASIP J. on Applied Signal Process.*, vol. 2005, no. 6, pp. 972–980, May 2005.

[2] M. C. Valenti and B. D. Woerner, "Iterative channel estimation and decoding of pilot symbol assisted turbo codes over flat-fading channels," *IEEE J. Sel. Areas Commun.*, vol. 19, no. 9, pp. 1697–1705, Sep. 2001.

[3] L. Schmitt, "On iterative receiver algorithms for concatenated codes," Ph.D. dissertation, Institute for Integrated Signal Processing Systems, RWTH Aachen University, Aachen, Germany, Mar. 2008.

[4] F. Sanzi, S. Jelting, and J. Speidel, "A comparative study of iterative channel estimators for mobile OFDM systems," *IEEE Trans. Wireless Commun.*, vol. 2, no. 5, pp. 849–859, Sep. 2003.

[5] G. Auer and J. Bonnet, "Threshold controlled iterative channel estimation for coded OFDM," in *IEEE Veh. Technol. Conf.*, Dublin, Ireland, Apr. 2007.

[6] S. ten Brink, "Convergence behavior of iteratively decoded parallel concatenated codes," *IEEE Trans. Commun.*, vol. 49, no. 10, pp. 1727–1737, Oct. 2001.

[7] Y. Huang and J. A. Ritcey, "Joint iterative channel estimation and decoding for bit-interleaved coded modulation over correlated fading channels," *IEEE Trans. Wireless Commun.*, vol. 4, no. 5, pp. 2549–2558, Sept. 2005.

[8] S. M. Kay, *Fundamentals of Statistical Signal Processing, Volume I: Estimation Theory*. Prentice Hall PTR, 1993.

[9] J. K. Cavers, "An analysis of pilot symbol assisted modulation for rayleigh fading channels," *IEEE Trans. Veh. Technol.*, vol. 40, no. 4, pp. 686–693, Nov. 1991.

[10] H. Meyr, M. Moeneclaey, and S. Fechtel, *Digital Communication Receivers: Synchronization, Channel Estimation and Signal Processing*, 1st ed. New York, NY: John Wiley & Sons, Inc., 1998.

[11] J. Baltersee, G. Fock, and H. Meyr, "An information theoretic foundation of synchronized detection," *IEEE Trans. Commun.*, vol. 49, no. 12, pp. 2115–2123, Dec. 2001.

[12] I. S. Gradstein, I. M. Ryshik, *Summen-, Produkt- und Integraltafeln, Band 1+2*, 5th ed. Thun, Frankfurt/M, Germany: Verlag Harri Deutsch, 1981.

[13] T. Clevorn, S. Godtmann, and P. Vary, "BER prediction using EXIT charts for BICM with iterative decoding," *IEEE Commun. Lett.*, vol. 10, no. 1, pp. 49–51, Jan. 2006.